◆ Human Brain Mapping 38:541–560 (2017) ◆

The Neurobiology of Emotion Regulation in Posttraumatic Stress Disorder: Amygdala Downregulation via Real-Time fMRI Neurofeedback

**Andrew A. Nicholson,[1,2,3] Daniela Rabellino,[2,3] Maria Densmore,[3] Paul A. Frewen,[1,4] Christian Paret,[5,6] Rosemarie Kluetsch,[6] Christian Schmahl,[6] Jean Théberge,[2,3,7,8,9] Richard W.J. Neufeld,[1,2,4] Margaret C. McKinnon,[10,11] Jim Reiss,[2] Rakesh Jetly,[12] and Ruth A. Lanius[1,2,3]*

[1]Department of Neuroscience, Western University, London, Ontario, Canada
[2]Department of Psychiatry, Western University, London, Ontario, Canada
[3]Department of Imaging, Lawson Health Research Institute, London, Ontario, Canada
[4]Department of Psychology, Western University, London, Ontario, Canada
[5]Department of Neuroimaging, Central Institute of Mental Health Mannheim, Medical, Faculty Mannheim/Heidelberg University, Heidelberg, Germany
[6]Department of Psychosomatic Medicine and Psychotherapy, Central Institute of Mental Health Mannheim, Medical Faculty Mannheim/Heidelberg University, Heidelberg, Germany
[7]Department of Medical Imaging, Western University, London, Ontario, Canada
[8]Department of, Medial Biophysics, Western University, London, Ontario, Canada
[9]Department of Diagnostic Imaging, St. Joseph's Healthcare, London, Ontario, Canada
[10]Mood Disorders Program and Clinical Neuropsychology Service, St. Joseph's Healthcare, Hamilton, Ontario, Canada
[11]Department of Psychiatry and Behavioural Neuroscience, McMaster University, Hamilton, Ontario, Canada
[12]Canadian Forces, Health Services, Ottawa, Ontario, Canada

Abstract: Amygdala dysregulation has been shown to be central to the pathophysiology of posttraumatic stress disorder (PTSD) representing a critical treatment target. Here, amygdala downregulation was targeted using real-time fMRI neurofeedback (rt-fMRI-nf) in patients with PTSD, allowing us to examine further the regulation of emotional states during symptom provocation. Patients ($n = 10$)

Additional Supporting Information may be found in the online version of this article.

Contract grant sponsor: Canadian Institutes of Health Research (CIHR), General Dynamics Land Systems, and the Canadian Institute for Veteran Health Research (CIMVHR)
Corrections added on 23 September 2016 after first online publication.

*Correspondence to: Ruth A. Lanius; University Hospital, Windermere Road, PO Box 5339, London, ON N6A 5A5, Canada. E-mail: Ruth.lanius@lhsc.on.ca
Daniela Rabellino is the shared first author.

The authors declare that they have no conflicts of interest.
Furthermore, this study is original research that has not been previously published or submitted for publication elsewhere.
Received for publication 3 June 2016; Revised 31 August 2016; Accepted 31 August 2016.
DOI: 10.1002/hbm.23402
Published online 20 September 2016 in Wiley Online Library (wileyonlinelibrary.com).

completed three sessions of rt-fMRI-nf with the instruction to downregulate activation in the amygdala, while viewing personalized trauma words. Amygdala downregulation was assessed by contrasting (a) *regulate* trials, with (b) *viewing* trauma words and not attempting to regulate. Training was followed by one transfer run not involving neurofeedback. Generalized psychophysiological interaction (gPPI) and dynamic causal modeling (DCM) analyses were also computed to explore task-based functional connectivity and causal structure, respectively. It was found that PTSD patients were able to successfully downregulate both right and left amygdala activation, showing sustained effects within the transfer run. Increased activation in the dorsolateral and ventrolateral prefrontal cortex (PFC), regions related to emotion regulation, was observed during *regulate* as compared with *view* conditions. Importantly, activation in the PFC, rostral anterior cingulate cortex, and the insula, were negatively correlated to PTSD dissociative symptoms in the transfer run. Increased functional connectivity between the amygdala- and both the dorsolateral and dorsomedial PFC was found during *regulate*, as compared with *view* conditions during neurofeedback training. Finally, our DCM analysis exploring directional structure suggested that amygdala downregulation involves both top-down and bottom-up information flow with regard to observed PFC-amygdala connectivity. This is the first demonstration of successful downregulation of the amygdala using rt-fMRI-nf in PTSD, which was critically sustained in a subsequent transfer run without neurofeedback, and corresponded to increased connectivity with prefrontal regions involved in emotion regulation during the intervention. *Hum Brain Mapp 38:541–560, 2017*.

Key words: fMRI neurofeedback; posttraumatic stress disorder; amygdala; emotion; brain connectivity

INTRODUCTION

It has been well documented that dysregulation of amygdala neural circuitry—a brain region associated with the generation and processing of emotions [Duvarci and Pare, 2014; Frank et al., 2014; LeDoux, 2007]—is central to the development and maintenance of symptoms experienced by patients with posttraumatic stress disorder (PTSD) [Aghajani et al., 2016; Birn et al., 2014; Etkin and Wager, 2007; Lanius et al. 2010, 2015; Mickleborough et al., 2011; Patel et al., 2012; Pitman et al., 2012; Shin and Liberzon, 2010; Stevens et al., 2013; Weston, 2014; Yehuda et al., 2015]. The amygdala, along with the prefrontal cortex (PFC), a region central to emotion regulation [Etkin et al., 2011, 2015], displays unique activation patterns among PTSD patients across a number of modalities, including symptom provocation [Frewen et al., 2011; Hayes et al., 2012; Hopper et al., 2007], fear processing [Bruce et al., 2013; Bryant et al., 2008; Williams et al., 2006; Wolf and Herringa, 2016; Zhu et al., 2016], and resting state [Brown et al., 2014; Huang et al., 2014; Koch et al., 2016; Nicholson et al., 2015]. Critically, during rest, the amygdala also displays altered connectivity to the cingulate cortex [Brown et al., 2014; Nicholson et al., 2015; Sripada et al., 2012], insula [Fonzo et al., 2010; Nicholson et al., 2016a; Rabinak et al., 2011; Sripada et al., 2012] and PFC [Birn et al., 2014; Brown et al., 2014; Nicholson et al., 2015; Stevens et al., 2013] among patients with PTSD.

Notably, heightened symptoms of hyperarousal in PTSD are correlated with negative medial PFC-amygdala coupling [Sadeh et al., 2014], and hyper/hypo-activation of the amygdala and medial PFC, respectively, during emotional processing [Bruce et al., 2013]. This pattern of findings points towards attenuated top-down inhibition from the PFC and rostral anterior cingulate (ACC) on the amygdala in PTSD patients, leading to hyperactivation of the limbic system, contributing to the emotion dysregulation observed in the disorder [Admon et al., 2013; Aupperle et al., 2012; Lanius et al., 2010; Pitman et al., 2012; Ronzoni et al., 2016; Shin and Liberzon, 2010]. Accordingly, it has been suggested that downregulation of the amygdala through recruitment of emotion regulatory resources from the PFC may represent a potential treatment for patients with PTSD [Doll et al., 2016; Koch et al., 2016]. Indeed, the efficacy of electroencephalography neurofeedback (EEG-nf) targeting these regions has already been illustrated [Kluetsch et al., 2014; Reiter et al., 2016]. Here, EEG-nf has been shown to plastically modify the aforementioned neural circuitry mediating PTSD, leading to acute symptom alleviation [Kluetsch et al., 2014]. Specifically, one 30-minute session of alpha desynchronizing EEG-nf was shown to shift amygdala complex connectivity away from fear/defense processing and memory regions towards prefrontal emotion regulation areas after intervention [Nicholson et al., 2016b]. In contrast to EEG-nf, real-time fMRI neurofeedback (rt-fMRI-nf) offers enhanced spatial resolution thereby increasing potential for targeted treatment. To date however, rt-fMRI-nf has not been utilized with PTSD patients to investigate and normalize aberrant amygdala activity/connectivity.

Rt-fMRI-nf utilizes a brain-computer interface to process and feedback real-time BOLD signal activation in a region-of-interest (ROI) to individuals inside the scanner. Ergo, participants are presented with online information that corresponds to their success in regulating the ROI. This neuroimaging method allows for the exploration of neural mechanisms that

underlie concomitant shifts in performance due to feedback training [Sitaram et al., 2007]. Several studies have examined the capacity to regulate emotions by targeting neurofeedback of the amygdala using rt-fMRI-nf, in healthy individuals [Brühl et al., 2014; Keynan et al., 2016; Paret et al., 2014, 2016b; Zotev et al., 2011] as well as in psychiatric populations, including borderline personality disorder (BPD) [Paret et al., 2016a], and major depressive disorder [Young et al., 2014; Zotev et al., 2016]. In support of this concept, self-regulation of the amygdala as compared with sham regions via rt-fMRI-nf has been shown to concomitantly affect activation in PFC areas involved in emotion regulation, as well as enhance amygdala-PFC connectivity [Koush et al., 2013; Paret et al., 2014; 2016b; Zotev et al., 2011] and amygdala-rostral ACC coupling [Zotev et al., 2011]. Similarly, using rt-fMRI-nf to target the regulation of the lateral PFC during cognitive reappraisal resulted in decreased amygdala BOLD response [Sarkheil et al., 2015]. Moreover, active pain coping through rt-fMRI-nf was associated with increased activity in the PFC and ACC [Emmert et al., 2016]. Critically, in a feasibility rt-fMRI amygdala downregulation study, involving three patients with PTSD [Gerin et al, 2016], patients reported an acute decrease in symptoms along with a concatenate normalization of brain connectivity, albeit, explicit amygdala downregulation was not reported.

The aim of the present study was therefore to investigate the ability of PTSD patients to self-regulate PTSD-related emotional states by utilizing rt-fMRI-nf to downregulate the amygdala. An additional aim was to better understand the neural connectivity underlying the psychopathology of this disorder by use of online emotion regulation. We predicted that exposure to personalized trauma words while downregulating the amygdala would recruit prefrontal emotion regulation regions (dorsolateral and ventrolateral) [Etkin et al., 2015] as compared to simply viewing personalized trauma words. Moreover, we predicted that during neurofeedback training, amygdala connectivity to the same PFC regions would be strengthened. Finally, we predicted that activation of the PFC, rostral ACC and insula would be correlated to state PTSD symptoms during neurofeedback training.

METHODS

Participants

The sample consisted of $n = 10$ PTSD patients (see Table I for demographic and clinical information). Participants were recruited in 2015 through flyers and clinician referrals. Exclusion criteria for participants with PTSD included: noncompliance with 3T fMRI safety standards, a history of head injury with loss of consciousness, significant untreated medical illness, neurological disorders, pervasive developmental disorders, and pregnancy. Further clinical exclusion criteria for PTSD patients included a history of bipolar disorder or schizophrenia, and alcohol or substance dependence/abuse not in sustained full remission within 6 months prior to participation in the study. Participants were assessed using the DSM-IV Structured Clinical Interview (SCID) [First et al., 1997], the Clinical Administered PTSD Scale (CAPS-5) [Blake et al., 1995], Beck's Depression Inventory (BDI) [Beck et al., 1997], the Childhood Trauma Questionnaire (CTQ) [Bernstein et al., 2003], and the Multiscale Dissociation Inventory (MDI) [Briere et al., 2005]. In addition, to assess state changes in PTSD and dissociative symptoms, participants completed the Response to Script Driven Imagery (RSDI) Scale [Hopper et al., 2007] after each of the four fMRI runs, which consisted of the following subscales: dissociation, hyperarousal, avoidance, and reliving. All scanning took place at the Lawson Health Research Institute in London, Ontario, Canada. The research ethics board at the University of Western Ontario approved the current study, and all participants provided written informed consent.

TABLE I. Demographic and clinical information

Measure	PTSD ($n = 10$)
Age	$M = 49.6 \pm 6.5$
Sex	Females = 6
CAPS Severity	32.2 ± 9.6
CTQ	56.7 ± 25.8
BDI	27.1 ± 14.4
MDI-DENG	15.1 ± 5.0
MDI-DEPR	11.1 ± 7.0
MDI-DERL	11.6 ± 6.6
MDI-ECON	13.3 ± 5.0
MDI-MEMD	11.8 ± 5.8
MDI-DDIS	9 ± 5.8
Current medication	$n = 9$

Abbreviations: CAPS, Clinician Administered PTSD Scale; CTQ, Childhood Trauma Questionnaire; BDI, Becks Depression Inventory; MDI, Multiscale Dissociation Inventory; DENG, Disengagement; DEPR, Depersonalization; DERL, Derealization; ECON, Emotional Constriction; MEMD, Memory Disturbance; IDDID, Identity Dissociation.

Experimental Conditions, Visual Feedback, and Instructions

Participants were instructed to "regulate the feeling center of their brain," referencing the role of this region (referring to the amygdala) to the perception and processing of emotions. In order to elicit unbiased regulatory strategies, specific instructions on how to regulate the brain region-of-interest (ROI) was not provided. During training trials, neurofeedback of the amygdala was displayed in the form of two identical thermometers on the left and right side of the screen inside the scanner (to ensure high visibility), where the bars on the thermometer increased or decreased as BOLD signal increased versus decreased in the amygdala respectively. Patients were told that the orange line

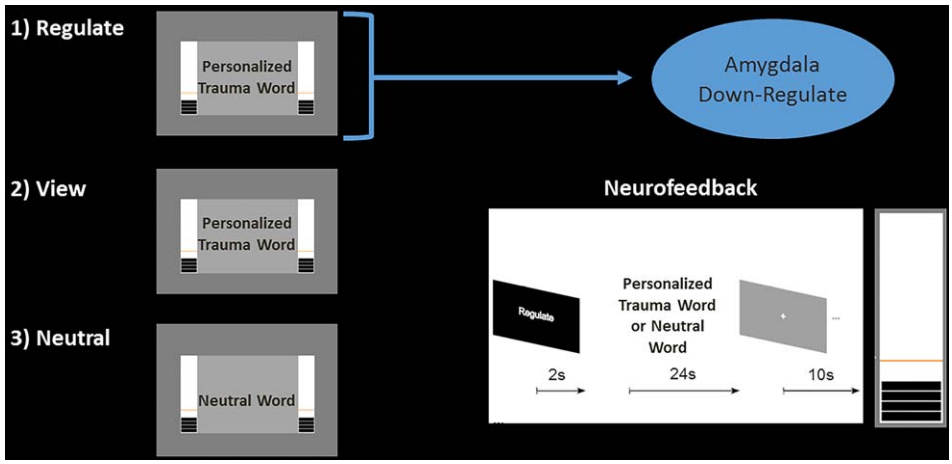

Figure 1.

Real-time fMRI amygdala neurofeedback experimental design. Participants were only instructed to downregulate neurofeedback thermometer bars, corresponding to amygdala activation, on regulate trials. Condition duration was 24 s, with 2 s of instructions prior. Personalized trauma words were presented in the scanner for regulate and view conditions, while neutral words were presented for the neutral conditions only. [Color figure can be viewed at wileyonlinelibrary.com.]

within the thermometer indicated the activation level in the ROI at rest (see Fig. 1). Participants were provided with written instructions, followed by a sham example within the scanner to ensure that they understood the task.

Our experiment consisted of three conditions (i) *regulate*, (ii) *view*, and (iii) *neutral* (see Fig. 1). During the *regulate* condition, patients were asked to decrease activity in the ROI (decrease bars on the thermometer corresponding to the amygdala), while viewing a personalized trauma word according to standard methods [Rabellino et al., 2015a, b]. During the *view* condition, patients were asked to refrain from regulating the thermometer bars and to simply view their personalized trauma word. During the *neutral* condition, patients were simply presented with a personalized neutral word, and also asked to refrain from regulating the bars. Trials were separated by an inter-trial fixation cross interval. Our experimental design consisted of three consecutive neurofeedback training runs, and one transfer run in which patients received the same three conditions albeit without neurofeedback from the thermometer (to assess learning effects immediately after training). An experimental run lasted about 9 minutes, consisting of 15 trials (5 of each condition, counterbalanced). Personalized trauma and neutral words were matched on subjective units of distress to control for between subject variability. Stimuli were presented with Presentation software (Neurobehavioral Systems, Berkeley, CA).

One bar on the thermometer display corresponded to 0.2% signal change in the amygdala. Here, the orange line (baseline), divided the thermometer into an upper activation range (maximum 2.8% signal changes) and a lower activation range (maximum 1.2% signal change) [Paret et al., 2014; 2016b; Zotev et al., 2011]. In order to circumvent regulation by avoiding the trauma word and directing attention to the thermometers, participants were asked to visually focus on the word during its entire presentation, and to view the two thermometers in their peripheral vision. Participants were also informed of the temporal delay that would occur during neurofeedback, corresponding to the BOLD signal delay. Finally, when a neurofeedback run was completed, patients were asked to rate their perceived ability to regulate their emotion center.

Delineation and BOLD Processing of the Amygdala for Real-Time Neurofeedback

In order to present amygdala neural activity to patients in real-time through the thermometer display, anatomical scans were first imported into BrainVoyager (version QX2.4, Brain Innovations, Maastrict, Netherlands), then skull-stripped and transformed into Talairach space. Subsequently, normalization parameters were loaded into TurboBrainVoyager (TBV) (version 3.0, Brain Innovations, Maastricht, Netherlands). Motion correction features and spatial smoothing using a 4-mm full-width-half-maximum (FWHM) Gaussian kernel were implemented in TBV, and the initial 2 volumes of the functional scans were discarded before real-time processing. An anatomical mask of the bilateral amygdala was then loaded, and the "best voxel selection" tool was used in TBV to calculate the BOLD signal amplitude of the ROI. This method identified the 33% of voxels with the highest beta-values for the *view > neutral* contrast. As previously outlined by Paret et al., [2014; 2016b], the voxels were dynamically determined based on (a) the voxel with the largest beta value, and (b) on

the magnitude of deviation from the mean of all condition betas [Goebel, 2014]. This feature ensured that there was no difference in the number of voxels used for signal extraction between subjects and was used to counterbalance moderate shifts in the anatomical delineation due to alignment errors across runs/movement-related slice shifts. The first two trials of each neurofeedback run consisted of *view* and *neutral* conditions in order to permit an initial selection of voxels based on the *view* > *neutral* contrast, which was updated as voxels were dynamically refined along the course of training.

Amygdala BOLD signal amplitude was passed to Presentation when a new volume had been processed. Latency of the feedback was equal to the TR (2 s) plus the time needed for real-time calculation/visual display by the presentation software (about half a second). For each trial, the mean of the last four data points before stimuli onset were taken as a baseline. The signal was smoothed by calculating the mean of the current and the preceding three data points [Paret et al., 2014, 2016b].

fMRI Image Acquisition

We utilized a 3 Tesla MRI Scanner (Trio, Siemens Medical Solutions, Erlangen, Germany) with a 32 channel head coil for brain imaging. Functional whole brain images of the BOLD contrast were acquired with a gradient echo T2* weighted echo-planar-imaging sequence (TE = 30 ms, TR = 2 s, FOV = 192 × 192 mm, flip angle = 80°, inplane resolution = 3 × 3 mm). One volume comprised 36 ascending interleaved slices tilted −20° from AC-PC orientation with a thickness of 3 mm and slice gap of 1 mm. Participants' heads were stabilized. The experimental runs comprised 284 volumes each, where T1-weighted anatomical images were acquired with a Magnetization Prepared Rapid Acquisition Gradient Echo sequence (TE = 3.03 ms, TR = 2.3 s, 192 slices and FOV = 256 × 256 mm).

fMRI Preprocessing

Preprocessing of the functional images was conducted with SPM12 (Wellcome Department of Cognitive Neurology, London, United Kingdom). After discarding the four initial volumes, the standard preprocessing routine included slice time correction to the middle slice, followed by spatial alignment to the mean image using a rigid body transformation, reslicing, and coregistration of the functional mean image to the anatomical. We then performed segmentation of all tissue types, and normalization to the Montreal Neurological Institute (MNI) standard template. Images were then smoothed using a 6 mm kernel FWHM. Additional correction for motion was implemented using the ART software package (www.nitrc.org/projects/artifact_detect), which computes regressors that account for outlier volumes, in addition to the six movement regressors computed during standard realignment in general linear modeling.

Statistical Analyses

First level analysis

The three neurofeedback runs and the transfer run were defined as separate sessions, and all events were modeled as blocks of brain activation and convolved with the hemodynamic response function. Here, ART software computations were included as nuisance variables to account for movement artifacts. Scans in the experiment corresponding to the instruction phase and initial baseline were also modeled. All experimental conditions were modeled separately; we also generated the *t*-contrast *regulate* > *view* on the first level.

Online region of interest amygdala downregulation analysis

In order to determine if participants were successfully able to downregulate amygdala activation using real-time fMRI neurofeedback, we investigated parameter estimates of the left and right amygdala during the *regulate* and *view* condition. Parameter estimates were extracted and graphed using rfx-plot software [Gläscher, 2009] via anatomical definition from the PickAtlas toolbox [Maldjian et al., 2003]. Extracted values were passed to SPSS version 20 for statistical analyses, where we computed a 3 (neurofeedback run) × 2 (condition) × 12 (2 s time bins across the 24 s condition) randomized block analysis of variance (ANOVA) for each amygdala hemisphere. We included time as a factor in the ANOVA, as we a-priori hypothesized that participants would be able to better regulate during the middle-end of the *regulate* condition as opposed to the beginning where patients are only beginning to learn how to regulate their amygdala activity.

We specified a-priori directional hypotheses, such that we expected amygdala activation to be lower across training runs and the transfer run during the *regulate* as compared with *view* condition. Therefore, we computed paired-sample *t*-tests for amygdala parameter estimates during the *regulate* as compared with the *view* condition, during the training and transfer runs separately for each amygdala hemisphere. We conducted the same paired sample *t*-tests on the middle-end (i.e., 8–24 s) of the condition, as again, we predicted that patients would be more successful in amygdala downregulation toward the end of the condition. In order to be statistically conservative, we implemented a Bonferroni correction for multiple comparisons for all paired-sample *t*-tests.

Offline analysis of brain activation during neurofeedback and transfer run

In addition to investigating amygdala downregulation during neurofeedback, we had previously defined 4 a-prior ROIs, including the dlPFC, vlPFC, rostral ACC/mPFC and the insula, in which we wanted to observe

activation across conditions. These regions were chosen based on their involvement in emotion regulation and monitoring physiological condition with respect to emotion [Birn et al., 2014; Bruce et al., 2013; Craig, 2009; Etkin et al., 2011, 2015; Gasquoine, 2014; Kurth et al., 2010; Patel et al., 2012, 2015; Pitman et al., 2012; Sadeh et al., 2014; Stevens et al., 2013; Yehuda et al., 2015]. Coordinates for the bilateral dlPFC, left vlPFC, and rostral ACC/mPFC were taken from a meta-analysis focusing on neurocircuitry models of PTSD [Patel et al., 2012]: right dlPFC (40 54 6), left dlFPC (−26 20 42), left vlPFC (−24 54 −4), rostral ACC (2 26 22). Coordinates for the right vlPFC were taken from Paret et al. [2016b], where this region was shown to be recruited during the downregulation of the amygdala in a healthy female sample: right vlPFC (54 41 1). We used PickAtlas to define 15mm radius spheres around the dlPFC, vlPFC, and rostral ACC/mPFC coordinates, where 6 mm spheres were defined separately for insula subregions [Ichesco et al., 2014] extracted using standard coordinates from previous anatomical and MR imaging studies [Ichesco et al., 2014; Taylor et al., 2009]: bilateral anterior insula (left = −32, 16, 6; right = 32, 16, 6), bilateral mid insula (left = −38, 2, 8; right = 38, 2, 8), and bilateral posterior insula (left = −39, −15, 1; right = 39, −15, 8). Insula subregions were examined separately as they have been shown to display unique connectivity in PTSD patients [Nicholson et al., 2016a] and orchestrate differential functions with regard to interoception [Craig, 2009], where a smaller radius was used to investigate subregions separately. All coordinates reported were in MNI space. We generated two simple masks for ROI data analyses, the first contained only the dlPFC and vlPFC spheres, as we hypothesized these to be the most influential regions during amygdala down regulation. The second mask contained all ROIs (dlPFC, vlPFC, rostral ACC, and insula subregions), which was only used for correlations with symptoms.

In order to verify that these 4 a-priori regions were in fact important in learning to downregulate amygdala activation, we checked to see if they were also identified in a conservative FDR-corrected 3 (condition) × 3 (neurofeedback training run) repeated measures ANOVA, investigating whole brain activation (FDR cluster-corrected $P < 0.05$ $k = 10$). Hence, our results are both hypothesis and data driven (corrected for multiple comparisons).

Next, to specifically test our hypothesis regarding regions recruited during amygdala downregulation, we analyzed two different one-way ANOVAs (1) including only the training runs, (2) including the training runs and transfer run, for the contrast *regulate* > *view*. For this ROI analysis, we applied the PFC mask only.

RSDI and trait symptom correlation analyses

In order to characterize neural mechanisms relating emotion regulation to PTSD symptom presentation, we conducted a regression analysis for both the amygdala online analysis and ROI offline analysis. Here, we correlated state changes in PTSD symptoms collected for each run to neural activation during the *regulate* as compared with the *view* condition, via a multiple regression analyses. We correlated RSDI subscales to amygdala and a-priori ROI activation during the training runs and the transfer run. These analyses utilized the aforementioned error protection rate for multiple comparisons, and we only applied the ROI mask containing all ROIs (dlPFC, vlPFC, rostral ACC, and insula subregions). We also computed a repeated measures ANOVA to investigate how RSDI state scores fluctuate across training and transfer runs. In addition, we correlated trait PTSD symptom severity (CAPS total scores) to individual patient's ability to downregulate the amygdala during the neurofeedback training runs and the transfer run, using a Pearson's bivariate correlation.

Offline generalized psychophysiological interaction (gPPI) analysis

First level gPPI analysis.. Here, our objective was to observe changes in task-dependent amygdala connectivity during neurofeedback training. The general psychophysiological interaction (gPPI) method allows one to study task-dependent functional connectivity in more than two task conditions [McLaren et al., 2012]. Resulting parameter estimates can then be interpreted as the condition-specific functional connectivity of the seed region to a target region. Hence, gPPI allows us to understand how brain regions interact in a task-dependent manner. We followed standard a gPPI analysis protocol [McLaren et al., 2012], which has been previously published with regard to amygdala connectivity by Paret et al. [2016b] and Kerr et al. [2012] Task regressors—*regulate*, *view*, and *neutral*—were convolved with the standard hemodynamic response function. Amygdala seeds were defined using the anatomical atlas from PickAtlas, where the signal time course was extracted for the left and right amygdala separately, for each of the three training runs. For amygdala ROIs, a model was computed defining the psychological task regressor, the psychological regressor of amygdala signal time course, and the interaction terms. The PPI regressor was deconvolved before modeling, and movement was corrected for using ART software. The beta coefficients for the interaction terms regulate, view, and neutral were passed forward to analyze on the group level. First level analyses were performed individually for each of the neurofeedback training.

Second level gPPI analysis.. We computed a 3 (run) × 3 (condition) repeated measures ANOVA for both amygdala seed regions. We investigated gray matter clusters for the run by condition interaction (FDR cluster-corrected $P < 0.05$, $k = 10$). To test specific hypotheses of areas showing increased amygdala connectivity during the *regulate* condition, we then conducted follow-up analyses on FDR-corrected clusters identified in the ANOVA, using paired

sample t-tests for the contrasts *regulate > view*, and *view > regulate*, separately for the left and right amygdala (FDR cluster-corrected $P < 0.05$, $k = 10$).

Offline dynamic causal modeling (DCM) analysis

To test directional information flow, complimenting the functional structure defined with our gPPI analysis, we computed a dynamic causal modeling (DCM) analysis [Friston et al., 2003]. The DCM approach takes a biophysiologically plausible model and aims to estimate, and make inferences about, the coupling among brain areas and how that coupling is influenced by changes in experimental context [Friston et al., 2003]. Via Bayesian inferences, DCM infers the probability that a given model fits the signal time course. Bayesian Model Selection (BMS) is used to define the best model based on its model evidence, relative to all other models defined in the analysis [Stephan et al., 2009, 2010].

We used our gPPI analysis to inform the delineation of the nodes in our models. Specifically, we investigated regions showing increased connectivity to the left and right amygdala for the *regulate > view* condition, which were the dlPFC and the vlPFC. Here, the dlPFC and vlPFC have also previously been shown to be implicated in emotion regulation [Etkin et al., 2011; Golkar et al., 2012; Paret et al., 2014, 2016b]. We tested a series of nine amygdala-PFC models published previously with regard to amygdala neurofeedback regulation [Paret et al., 2016b], which define bidirectional intrinsic connectivity between the amygdala and PFC. These models are also in keeping with the anatomical structure for the whole model space [Ghashghaei et al., 2007] (see Fig. 6). The signal associated with the experimental conditions enters the network either at the amygdala node, at the PFC node, or at both sites. The *regulate* condition was assumed to modulate amygdala-PFC connectivity in either bottom-up, top-down, or both directions. From each subject, the first eigenvariate of the signal time course was extracted from the bilateral anatomical amygdala, and the three PFC ROIs separately (radius = 6 mm). We optimized voxel selection by selecting peak activation voxels within the amygdala from the *view* condition, and selecting peak activation voxels within PFC ROIs from the *regulate* condition, based on the single-subject *t*-contrasts. Here, sphere centers were defined as the peak coordinates within the bilateral amygdala and the PFC regions. Interestingly, almost all of the participants displayed peak coordinates within the bilateral dorsal amygdala. In order to prevent inter-subject variations of amygdala subregions [Nicholson et al., 2015; Paret et al., 2016b; Roy et al., 2009], only dorsal amygdala coordinates were selected. After defining our bi-direction liner models on the subject level, models were then inverted, and exceedance probability assessed on the group level via random effects comparisons. We also computed a random effects family inference analysis, in order to first identify which family of models best fits the data. Here, we grouped models based on their driving inputs. Hence, we had three families of models: (1) models with both amygdala and PFC driving inputs (models 1–3), (2) models with amygdala driving inputs only (models 4–6), and (3) models with PFC driving inputs only (models 7–9) (Fig. 6).

RESULTS

Response to Script Driven Imagery Analysis

RSDI total scores were found to not differ significantly across training runs and the transfer run, when computing a repeated measures ANOVA for the main effect of run ($F(3, 27) = 0.495$, *ns*) in which sphericity was not violated.

Online Amygdala Neurofeedback

Regarding the right amygdala, the 3 (run) × 2 (condition) × 12 (2 s time bins across the 24 s condition) randomized ANOVA yielded a significant main effect of condition ($F(1, 9) = 109.80$, $P < 0.001$) and time ($F(12, 108) = 2.34$, $P < 0.05$), and also a significant condition × time interaction ($F(12, 108) = 2.68$, $P < 0.005$), where sphericity was not violated.

For the left amygdala, the 3 (run) × 2 (condition) × 12 (time bin) randomized ANOVA yielded a significant main effect of condition ($F(1, 9) = 31.68$, $P < 0.001$) and time ($F(12, 108) = 3.58$, $P < 0.001$), and also a significant condition × time interaction ($F(12, 108) = 2.16$, $P < 0.05$), where sphericity was also not violated. We found neither a significant main effect of run, nor any significant interactions with this variable, for both the right and left amygdala.

This justified the examination of our a-priori directional hypotheses. Here, we expected amygdala activation to be lower across training runs and the transfer run, during the *regulate* as compared with *view* condition. Furthermore, we predicted that participants would be better able to *regulate* towards the middle-end of the condition.

For the right amygdala, we observed significantly lower activation during the *regulate* as compared with the *view* condition across time bins for the three neurofeedback training runs ($t(11) = -3.86$, $P = 0.001$), and the transfer run ($t(11) = -3.64$, $P = 0.001$) (see Fig. 2a,c). The significance of these results were highlighted when considering only the last two thirds (8–24 s) of the time bins within the conditions for the three neurofeedback training runs ($t(7) = -10.67$, $P < 0.001$), and the transfer run ($t(7) = -6.55$, $P < 0.001$) (see Fig. 2a,c).

Similarly, for the left amygdala, we also observed significantly lower activation during the *regulate* as compared with *view* condition across time bins for the three neurofeedback training runs ($t(11) = -3.08$, $P = 0.004$), and the transfer run ($t(11) = -2.18$, $P < 0.025$), (see Fig. 2b,c). The significance of these results were also highlighted when considering only the last two thirds of the time bins within

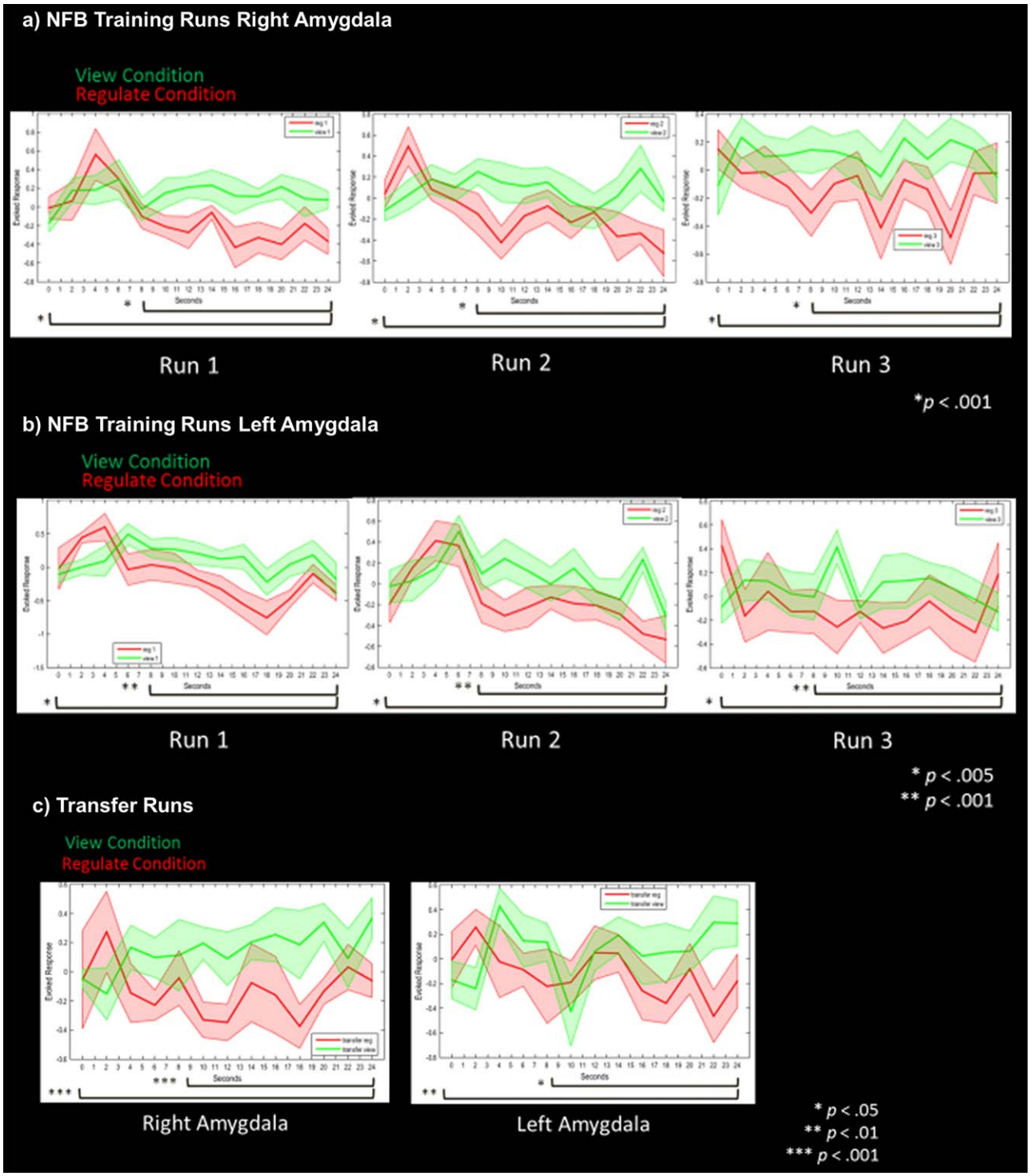

Figure 2.

(a) Right amygdala parameter estimates corresponding to amygdala activation during neurofeedback runs for the view (solid green line) and regulate (solid red line) conditions. (b) Left amygdala parameter estimates corresponding to amygdala activation during neurofeedback runs for the view (solid green line) and regulate (solid red line) conditions. (c) Bilateral amygdala parameter estimates corresponding to activation during the transfer run without neurofeedback for the view (solid green line) and regulate (solid red line) conditions. Shaded red and green regions adjacent to the solid lines indicate standard error of the mean. Statistical thresholds corresponds to a-priori paired sample *t*-tests, comparing amygdala activation during view versus regulate across the whole condition, and for the last two thirds of the condition. Each of these respective *t*-tests are indicated by the black bars on the bottom of each graph. Asterisks indicate Bonferroni corrected statistical thresholds for paired sample *t*-tests. Abbreviations: NFB, neurofeedback. [Color figure can be viewed at wileyonlinelibrary.com.]

TABLE II. One-way ANOVA for regulate > view prefrontal cortex analysis

Analysis	Gyrus/sulcus	H	BA	Cluster size	MNI coordinate x	y	z	$F(2, 27)$/ $F(3, 36)$	Z score	P FDR
Main Effect of Run, Across Training Runs	Dorsolateral PFC	L	9	412	−34	26	36	11.98	3.55	<0.05
	Dorsolateral PFC	R	10	1130	36	58	19	11.79	3.53	<0.001
	Ventrolateral PFC	R	11	1130	46	42	−7	9.24	3.13	<0.001
Main Effect of Run, Across Training Runs and Transfer	Ventrolateral PFC	R	45	1010	42	34	2	9.73	3.78	<0.001
	Dorsolateral PFC	R	46	1010	42	50	20	5.05	2.57	<0.001

One-way analysis of variance for offline activation during regulate as compared with view, for the 4 a-prior prefrontal cortex regions of interest (P-FDR corrected < 0.05, $k = 10$). Abbreviations: BA, Brodmann area; FDR, False discovery rate; H, hemisphere; PFC, prefrontal cortex.

the conditions, for the three neurofeedback training runs ($t(7) = -6.58$, $P < 0.001$), and the transfer run ($t(7) = -2.72$, $P < 0.01$) (see Fig. 2b,c).

Offline Whole Brain Activation

When investigating the whole brain FDR cluster-corrected repeated measures ANOVA, we found that all a-priori ROIs were significant for the main effect of run (dlPFC, vlPFC, rostral ACC, and insula subregion; see Supporting Information Table s1). The presence of our ROIs in a conservative FDR-corrected ANOVA supported their use in subsequent one-way ANOVAs investigating the a-priori *regulate > view* contrasts. Thus, our analysis may be viewed as both hypothesis and data driven (FDR cluster-corrected).

When investigating the one-way ANOVAs for the *regulate > view* contrasts, we found significant bilateral dlPFC (BA 9 and 10) and right vlPFC (BA 11) activation for the main effect of run across the neurofeedback training runs (see Table II; Fig. 3a). A similar pattern was found for the main effect of run when including the transfer run with the neurofeedback training runs, where we report significant activation in the right vlPFC (BA 45) and the right dlPFC (BA 46) (see Table II; Fig. 3b). We then conducted follow-up t-tests under the same error protection rate in order to observe effects of learning across the training trials and transfer run. We found significantly higher activation in the bilateral dlPFC (BA 10 and 9) and the right vlPFC (BA 47) in training run 3 as compared with training run 1, for the contrast *regulate > view* (see Table III; Fig. 3c). We did not find significantly increased activation in the transfer run as compared with run 1 for the contrast *regulate > view*.

RSDI and Trait Symptom Correlation Analyses

We found a significant negative correlation with state dissociation during the transfer run, to the rostral ACC, and left dlPFC BA 9, in addition to the bilateral anterior, mid and posterior insula (see Table IV; Fig. 4), for the regulate as compared with view condition. We did not find significant correlations (positive or negative) with activation during the neurofeedback training runs to state dissociation. Furthermore, we did not demonstrate significant correlations during the neurofeedback training runs and transfer run for reliving, hyperarousal, and avoidance. Additionally, we found that trait PTSD severity (CAPS total) was positively correlated to right amygdala downregulation, during neurofeedback training runs 1 ($r = 0.87$, $P < 0.001$) and 3 ($r = 0.70$, $P < 0.05$). We found non-significant correlations between CAPS total and left amygdala down regulation, as well as for right amygdala down-regulation and training run 2 and the transfer run.

gPPI Results

For the 3 (condition) × 3 (run) repeated measures ANOVA, we report a significant condition by run interaction for the right dlPFC (BA 46) and dorsomedial (dm)PFC (BA 9,8), right precuneus, bilateral cerebellar tonsil (lobule 8, 6), and right cuneus (see Table V). This supported our a-priori t-tests examining greater connectivity during the *regulate* as compared with the *view* condition across neurofeedback training runs.

On balance, we report increased left amygdala connectivity during the *regulate* condition as compared with the *view* condition, to the left dmPFC/dorsal ACC (BA 9) and the right dlPFC (BA 46) across neurofeedback training runs (see Table VI; Fig. 5a). Similarly, we found increased right amygdala connectivity during the *regulate* condition as compared with the *view* condition, to the right dmPFC (BA 8), across neurofeedback training runs (see Table VI; Fig. 5b).

DCM Results for Effective Connectivity

We tested nine previously published models for the left and right amygdala to the three PFC clusters identified in

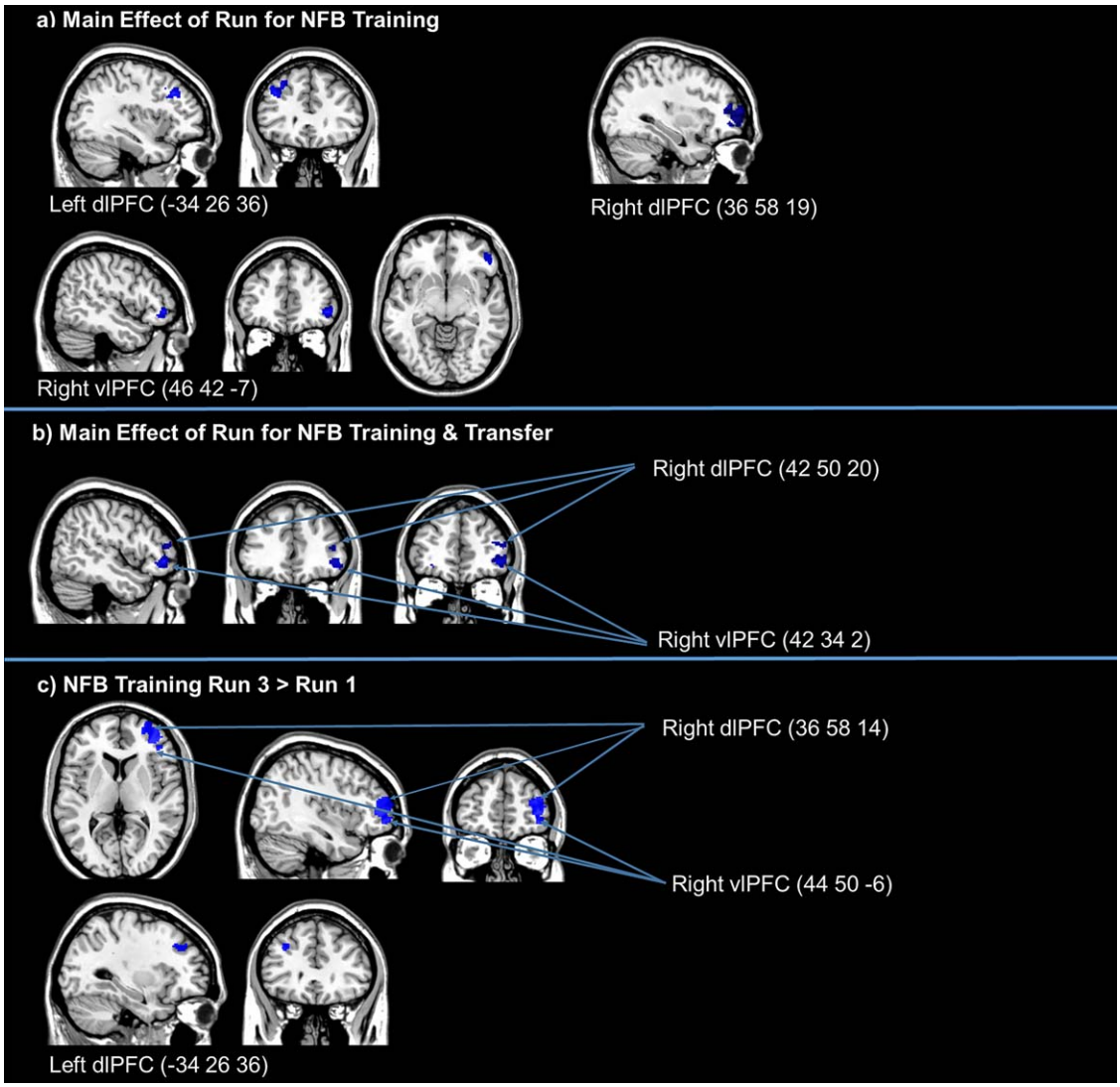

Figure 3.

(a) One-way ANOVA examining the main effect of run across neurofeedback training runs for regulate as compared view conditions (FDR-cluster-corrected $P < 0.05$, $k = 10$). (b) One-way ANOVA examining the main effect of run across neurofeedback training runs and the transfer run for regulate as compared with view conditions (FDR-cluster-corrected $P < 0.05$, $k = 10$). (c) Follow-up t-tests examining greater activation for regulate as compared with view conditions, for neurofeedback training run 3 as compared with run 1 (FDR-cluster-corrected $P < 0.05$, $k = 10$). Coordinates indicate x, y, z, in MNI space displayed in MRIcron software. Abbreviations: NFB, neurofeedback; dlPFC, dorsolateral prefrontal cortex; vlPFC, ventrolateral prefrontal cortex. [Color figure can be viewed at wileyonlinelibrary.com.]

the gPPI analysis, which is also supposed by anatomical studies of amygdala connectivity [Gasquoine, 2014]. For the left amygdala-right dlPFC models, there was a clear winner in terms of the family of models that best fit the data, where models with only PFC driving inputs (models 7–9) yielded an exceedance probability (xP) = 0.98 (see Fig. 6a). Furthermore, for the left amygdala-right dlPFC, we found a clear distinction for model 9, where our random effects analysis was in favor of the model characterized by network input to the dlPFC, with modulation of connectivity from the amygdala to the dlPFC (bottom-up) and from the dlPFC to the amygdala (top-down) by the *regulate* condition ($xP = 0.83$) (see Fig. 6a).

For the left amygdala-left dmPFC models, there was also a clear winner in terms of the family of models that best fit the data. Again, models with only PFC driving inputs (models 7–9) yielded an exceedance probability of $xP = 0.92$ (see Fig. 6b). For the left amygdala-left dmPFC,

TABLE III. Follow up *t*-test for regulate > view prefrontal cortex analysis

Analysis	Gyrus/sulcus	H	BA	Cluster size	MNI coordinate x	y	z	*T*(18)	*Z* score	*P FDR*
Run 3 > Run1	Dorsolateral PFC	R	10	1,407	36	58	14	4.86	4.08	<0.005
	Ventrolateral PFC	R	47	1,407	44	50	−6	4.01	3.52	<0.001
	Dorsolateral PFC	L	9	1,112	−34	26	36	4.83	4.06	<0.05
Transfer Run > Run 1	*ns*									

Follow-up *t*-test comparisons for the both the training and transfer + training one-way analyses of variance for the 4 a-prior prefrontal cortex regions of interest (*p*-FDR corrected < 0.05, $k = 10$). Abbreviations: BA, Brodmann area; FDR, False discovery rate; H, hemisphere; PFC, prefrontal cortex.

we report a less clear distinction for model 9 characterized by network input to the dmPFC and both bottom-up and top-down modulation by the *regulate* condition ($xP = 0.40$) (see Fig. 6b). However, it is important to note that models within the same family, models 7 and 8, also fit the data in a similar way, with $xP = 0.30$ and $xP = 0.25$, respectively. This result matches our finding that the family of models which best fits the data are those with PFC driving inputs only with an $xP = 0.92$.

Finally, for the right amygdala-right dmPFC models, there was a clear winner for the family inference analysis, where models with only PFC driving inputs had the highest exceedance probability ($xP = 0.98$) (see Fig. 6c). When examining models separately, model 9 was again the strongest, characterized by network input to the dmPFC and both bottom-up and top-down modulation by the *regulate* condition ($xP = 0.62$) (see Fig. 6c).

DISCUSSION

Emotion dysregulation is central to the clinical presentation of PTSD and is thought to arise, in part, due to attenuated amygdala top-down inhibition from the PFC [Aupperle et al., 2012; Lanius et al., 2010; Pitman et al., 2012; Ronzoni et al., 2016; Shin and Liberzon, 2010] . This aberrant amygdala activity/connectivity is illustrated in a number of studies where the majority of patients with PTSD are characterized by hyperactivation of the amygdala [Aghajani et al., 2016; Birn et al., 2014; Etkin and Wager, 2007; Lanius et al., 2010, 2015; Mickleborough et al., 2011; Patel et al., 2012; Pitman et al., 2012; Shin and Liberzon, 2010; Stevens et al., 2013; Weston, 2014; Yehuda et al., 2015; but also see the dissociative subtype of PTSD Lanius et al., 2010, 2015; Nicholson et al, 2015]. Accordingly, we sought to investigate the ability of patients to self-regulate their emotional states using utilizing rt-fMRI-nf targeting amygdala downregulation. An additional objective was to better understand PTSD neural connectivity as a function of real-time emotion regulation.

Here, we found that patients were able to successfully downregulate amygdala activity during trauma provocation, an effect that was sustained during the transfer run without neurofeedback. As predicted, the ability to downregulate the amygdala during neurofeedback and the transfer run was associated with increased activation in the dlPFC and vlPFC, regions associated with emotion regulation. In addition, the amygdala displayed increased task-based functional connectivity to the dlPFC and dmPFC during neurofeedback training, for the *regulate* as compared with *view* condition. In keeping with these findings, our DCM analysis suggested that amygdala-PFC connectivity is modulated by downregulation of the amygdala in both top-down and bottom-up directions, with driving

TABLE IV. PTSD symptom correlation to offline brain activation

Symptom	Analysis	Gyrus/sulcus	H	BA	Cluster size	MNI coordinate x	y	z	*T*(8)	*Z* score	P *FDR*
Dissociation	Negative Correlation, Transfer Run	Rostral ACC			1,194	2	34	28	18.53	5.38	<0.005
		Anterior, Mid and Posterior Insula	L		1,017	−38	−18	0	11.44	4.66	<0.005
		Anterior, Mid and Posterior Insula	R		1,116	38	14	−6	6.70	3.79	<0.005
		Dorsolateral PFC	L	9	726	−30	28	38	4.43	3.06	<0.05

Regression analysis with PTSD symptoms for the contrasts regulate> view, FDR-corrected gray matter clusters (*P*-FDR < 0.05, $k = 10$). Abbreviations: BA, Brodmann area; FDR,= False discovery rate corrected threshold; H, hemisphere; PFC, prefrontal cortex.

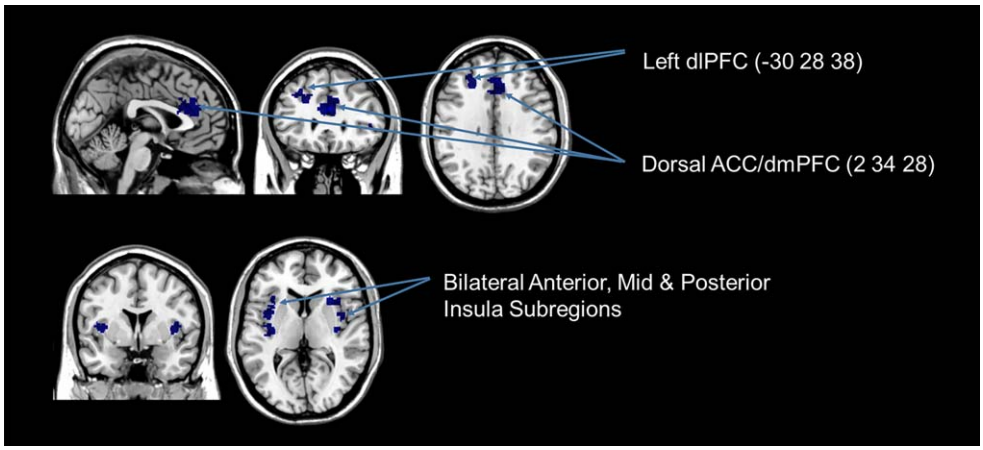

Figure 4.

Brain regions whose activation were negatively correlated to PTSD symptoms of dissociation during the transfer run, for the regulate as compared with view condition (FDR-cluster-corrected $P < 0.05$, $k = 10$). Coordinates indicate x, y, z, in MNI space displayed in MRIcron software. Abbreviations: dlPFC, dorsolateral prefrontal cortex; dmPFC, dorsomedial prefrontal cortex; vlPFC, ventrolateral prefrontal cortex; ACC, anterior cingulate cortex. [Color figure can be viewed at wileyonlinelibrary.com.]

inputs feeding directly into the PFC. Further, consistent with our predictions, we found that PFC, rostral ACC, and insula activation was correlated negatively to PTSD dissociative symptoms during the transfer run. Here, PTSD symptom severity positively correlated to the degree of amygdala downregulation during training runs 1 and 3, suggesting that patients with more severe PTSD symptoms actually decrease amygdala activity more during neurofeedback. Interestingly, these rt-fMRI results parallel those found with a different modality of neurofeedback (EEG), where one 30-minute session of alpha desynchronizing EEG-nf was shown to shift amygdala complex connectivity away from fear/defense processing and memory regions towards prefrontal emotion regulation areas after intervention [Nicholson et al., 2016b].

Amygdala Downregulation Success

We observed significantly decreased amygdala activation for the neurofeedback training runs and the transfer run, during the *regulate* as compared with *view* condition. Although several studies have examined the capacity to regulate emotions by targeting neurofeedback of the amygdala using rt-fMRI-nf, in healthy individuals [Brühl et al., 2014; Keynan et al., 2016; Paret et al., 2014, 2016b; Zotev et al., 2011], and in neuropsychiatric populations [Paret

TABLE V. The 3 (condition) × 3 (run) gPPI amygdala connectivity repeated measures ANOVA

					MNI coordinate					
Analysis	Gyrus/sulcus	H	BA	Cluster size	x	y	z	*F*(4, 81)	*Z* score	*P FDR*
Condition × Run Interaction	Dorsomedial PFC	L	9	344	−12	44	22	12.59	4.22	<0.001
	Precuneus	R	7	1,259	18	−48	52	12.37	4.18	<0.001
	Cerebellar Tonsil, Lobule 8	L		387	−22	−56	−42	12.96	4.23	<0.001
	Dorsomedial PFC	L	9	373	−26	38	44	12.65	4.23	<0.001
	Dorsolateral PFC	R	46	303	46	40	22	12.30	4.17	<0.001
	Cerebellum Declive, Posterior Lobe 6	R		417	26	−56	−22	12.26	4.16	<0.001
	Dorsomedial PFC	R	8	485	20	39	48	11.00	3.92	<0.001
	Cuneus	R	19	295	30	−84	32	10.88	3.89	<0.001

Repeated measures analysis of variance for the gPPI amygdala connectivity condition by run interaction, FDR-corrected gray matter clusters (P-FDR < 0.05, $k = 10$). Abbreviations: BA, Broadmann area; FDR, False discovery rate cluster-corrected threshold; H, hemisphere; PFC, prefrontal cortex.

TABLE VI. Follow-up paired *t*-test for regulate > view gPPI amygdala connectivity

Analysis	Gyrus/sulcus	H	BA	Cluster size	MNI coordinate			*T*(9)	*Z* score	*P FDR*
					x	y	z			
Left Amygdala Regulate> View	Left Dorsomedial PFC/ Dorsal ACC	L	9	81	−12	42	20	4.17	3.03	<0.05
	Right Dorsolateral PFC	R	46	48	50	40	24	4.36	3.12	<0.05
Right Amygdala Regulate> View	Right Dorsomedial PFC	R	8	74	18	38	48	4.12	3.01	<0.05

Paired sample *t*-tests for the gPPI amygdala connectivity analysis, for the contrast regulate> view, FDR-corrected gray matter clusters (*P*-FDR < 0.05, *k* = 10). Abbreviations: BA, Brodmann area; FDR, False discovery rate corrected threshold; H, hemisphere; PFC, prefrontal cortex.

et al., 2016a; Young et al., 2014; Zotev et al., 2014], this is the first study to demonstrate amygdala downregulation during trauma provocation among patients with PTSD. The significance of these results, surrounding both the neurofeedback training runs and the transfer run, was highlighted when comparing amygdala activation for the middle-end of each condition (8–24 s of the 24 s condition). Here, we speculate that patients require some time to successfully downregulate the amygdala after initially being presented with their trauma word, reflected in our findings of a small increase in amygdala activation at the beginning of the *regulate* condition. With regard to state PTSD symptoms, we did not find statistical differences in terms of RSDI scores across neurofeedback training runs and the transfer run. Additional studies are therefore required to assess PTSD symptoms as a function of repeated rt-FMRI-nf targeting amygdala downregulation.

Enhanced Activation in Emotion Regulation Regions During Amygdala Downregulation With Negative Correlations to PTSD Symptoms

When examining offline brain activation that occurred during the *regulate* compared with the *view* condition, we observed increased activation in emotion regulation PFC areas during the neurofeedback training runs and the transfer run. Specifically, we found a main effect of run

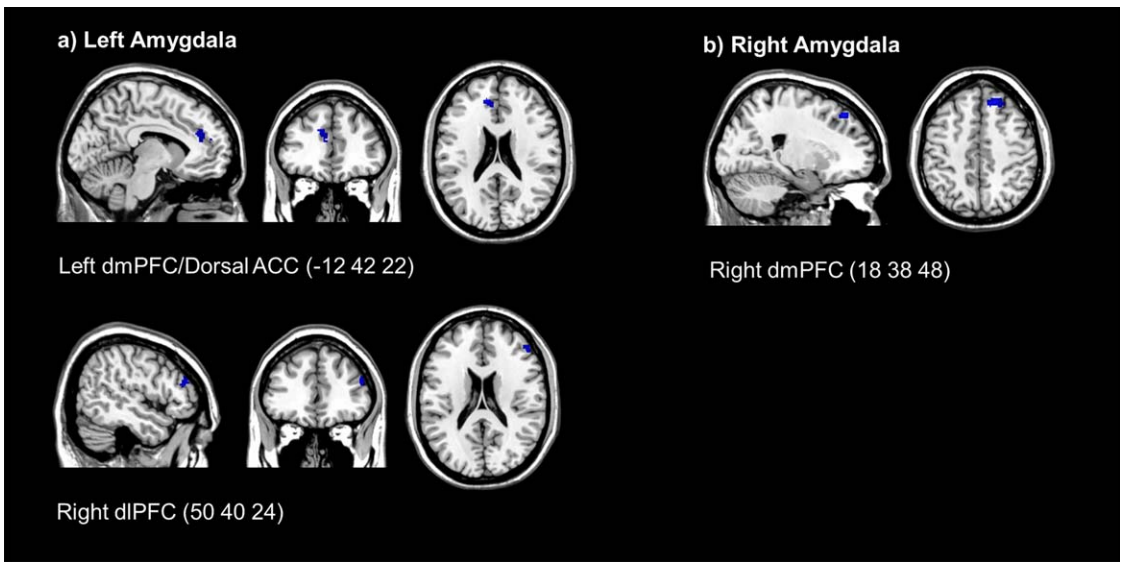

Figure 5.

(a) Increased task based functional connectivity during the neurofeedback regulate condition for the left amygdala. (b) Increased task based functional connectivity during the neurofeedback regulate condition for the right amygdala. (FDR-cluster-corrected $P < 0.05$, $k = 10$). Coordinates indicate x, y, z, in MNI space displayed in MRIcron software. Abbreviations: dlPFC, dorsolateral prefrontal cortex; dmPFC, dorsomedial prefrontal cortex; ACC, anterior cingulate cortex. [Color figure can be viewed at wileyonlinelibrary.com.]

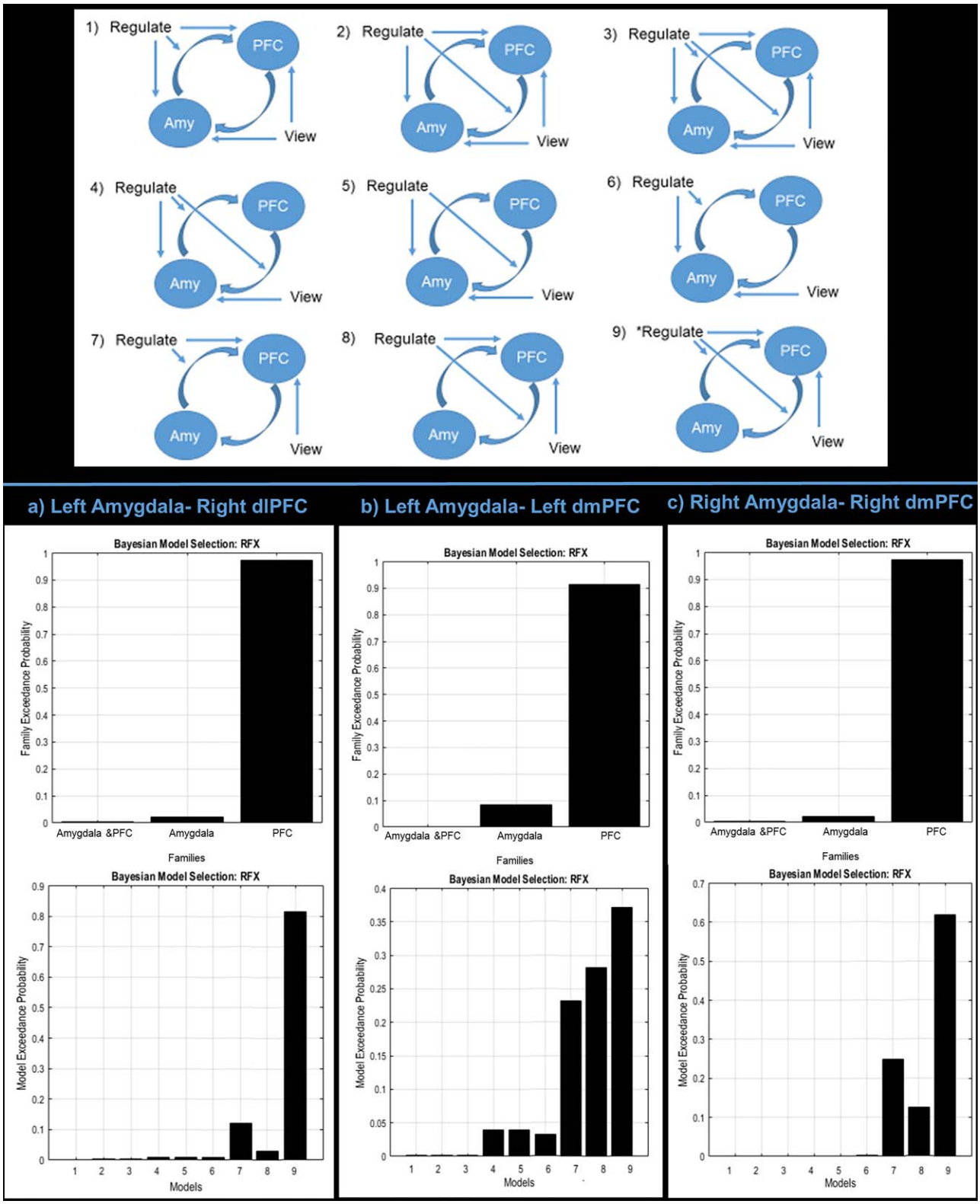

Figure 6.
(See legend on the next page.)

across the training runs for the *regulate > view* contrast in the bilateral dlPFC and right vlPFC. We also found a main effect of run for the *regulate > view* contrast across training runs and the transfer run in the right dlPFC and right vlPFC. Follow-up analyses revealed that there was stronger activation in the bilateral dlPFC and right vlPFC during run 3 as compared with run 1 for the *regulate > view* contrast. This suggests significant recruitment of emotion regulation regions as a function of learning to downregulate the amygdala during trauma triggers via neurofeedback. However, we did not observe significantly more PFC activation during the transfer run as compared with run 1 during the *regulate* as compared with *view* condition. Speculatively, the PFC may become more efficient with regard to regulating the amygdala by the transfer run, thereby yielding less detectable activation. This hypothesis is indirectly supported by the finding of decreased dissociation being correlated with PFC activation only during the transfer run and not the training runs. Alternatively, although patients were able to successfully downregulate their amygdala during the transfer run in which they did not receive neurofeedback, enhanced PFC activation during the transfer as compared with run 1 may require multiple neurofeedback training sessions

Our results parallel other pioneering proof-of-concept studies in the field, where self-regulation of the amygdala as compared with sham regions via rt-fMRI-nf was shown to concomitantly recruit activation in PFC regions associated with emotion regulation, as well as enhancing amygdala-PFC connectivity [Koush et al., 2013; Paret et al., 2014, 2016b; Zotev et al., 2011]. Inversely, using rt-fMRI-nf to target the regulation of the lateral PFC during cognitive reappraisal revealed a concomitant decrease in amygdala BOLD response [Sarkheil et al., 2015]. In a pattern of findings paralleling those observed for online emotion regulation, active pain coping through rt-fMRI-nf was associated with increased activity in the PFC and ACC [Emmert et al., 2016]. Similarly, Levesque et al. [2003] reported increased activation within the right dlPFC when healthy participants were asked to suppress negative emotions associated with increased amygdala activity. Finally, a recent review on the neural basis of emotion regulation [Etkin et al., 2015] highlights the dlPFC and vlPFC as key areas of explicit emotional regulation on emotional reactive regions, including the amygdala and periaqueductal gray. Thus, our study shows that amygdala downregulation using rt-fMRI-nf may be an effective means of enhancing PFC activity to regulate emotions, where increased PFC activation has also been reported when examining neural activity post treatment among PTSD patients [Peres et al., 2007; Ravindran and Stein, 2009; Seedat et al., 2004; Shin and Liberzon, 2010].

Our findings are further consistent with emotion modulation models of PTSD, which characterize PTSD symptom manifestation as a result of failed top-down inhibition of the PFC and rostral ACC on the amygdala in the majority of PTSD patients [Aupperle et al., 2012; Lanius et al., 2010; Patel et al., 2012; Pitman et al., 2012; Ronzoni et al., 2016; Shin and Liberzon, 2010]. In keeping with this hypothesis, PTSD symptoms of hyperarousal have been correlated with negative medial PFC-amygdala coupling [Sadeh et al., 2014], and hyper/hypo-activation of the amygdala and medial PFC, respectively, during PTSD emotional processing [Bruce et al., 2013]. Accordingly, downregulating the amygdala by recruiting emotion regulatory resources from the PFC may represent a potential treatment for patients with PTSD [Koch et al., 2016]. Critically, increased activation in the dlPFC, rostral ACC, and insula during the transfer run was negatively correlated to dissociative symptoms (emotional numbing, depersonalized, derealization, and disconnection). Here, the rostral ACC has been shown to resolve emotional conflict through top-down inhibition of the amygdala [Etkin et al., 2006]. Notably, the anterior, mid and posterior insula exhibit unique functions related to interoception, integrating bodily awareness with emotions and somatotopic representations, respectively [Critchley et al., 2004; Menon and Uddin, 2010; Pitman et al., 2012], have been shown to display altered activity and connectivity among PTSD patients [Lanius et al., 2010;

Figure 6.

Upper portion of figure indicates the nine models tested in the dynamic causal modeling analysis. Model number 9 was the best fitting model with respect to Bayesian model selection for all analyses examined. The nine models were derived from different combinations of signal input (either in the amygdala [amy], in the prefrontal cortex [PFC], or in both) and causal information flow (either from the amygdala to the PFC, from the PFC to the amygdala, or both). Models 1–9 are displayed with arrows indicating intrinsic information flow between the amygdala and PFC, and modulating input from the conditions ("regulate," "view") on the network nodes and connections. Referencing the bottom half of the figure, graphs on the top indicate the family level inference. Models were grouped in families based on their driving inputs (1) models with both amygdala and PFC driving inputs (models 1–3), (2) models with amygdala driving inputs only (models 4–6), and (3) models with PFC driving inputs only (models 7–9). The graphs on the lower half indicate the random effects analysis examining individual models not grouped into families. The exceedance probability (x*P*) of each model/family of models is displayed in vertical bars. Displayed are the exceedance probabilities for the family level inference (top) and individual model random effects analysis (bottom) for (a) the left amygdala-right dlPFC connection, (b) the left amygdala-left dmPFC connection, and (c) the right amygdala-right dmPFC connection. [Color figure can be viewed at wileyonlinelibrary.com.]

Nicholson et al., 2016a]. Furthermore, dissociation among patients with PTSD has been associated with poor interoception [Lanius et al., 2015]. Taken together, our results suggest that increased activation in emotion regulation regions and interoception/bodily awareness regions during the transfer run regulation are negatively correlated to dissociative symptoms. This pattern is similar to that observed in patients with BPD, where increased amygdala-PFC connectivity as a result of amygdala downregulation was negatively correlated, though not significantly, to symptoms of dissociation [Paret et al., 2016a].

Amygdala-PFC Functional Connectivity During Neurofeedback

We conducted a gPPI analysis to examine task-based functional connectivity as a result of neurofeedback training. In keeping with our hypotheses, we found increased connectivity between the left amygdala and the left dmPFC/dorsal ACC and right dlPFC, and increased connectivity between the right amygdala and the right dmPFC, during the *regulate* as compared with *view* condition. This finding indicates that when patients with PTSD are attempting to downregulate the amygdala, a concomitant increase in connectivity between the emotionally reactive amygdala and emotion regulatory dlPFC and dmPFC regions is observed [Admon et al., 2013; Etkin et al., 2011, 2015]. Our findings compliment previous work illustrating increased PFC connectivity during emotion regulation via rt-fMRI-nf [Koush et al., 2015; Zotev et al., 2011]. Notably, Scheinost et al. (2013) report increased resting-state connectivity of the dlPFC and decreased limbic network connectivity as a result of rt-fMRI-nf, which was associated with a change in contamination anxiety unique to the experimental group. Also utilizing gPPI, Kerr et al. [2012] report increased functional connectivity between the vmPFC and amygdala when patients had control over emotional stimuli, where the authors suggest vmPFC inhibition of amygdala processing involving emotional arousal/anticipation. In a related study, Banks et al. (2007) found increased dlPFC connectivity to the amygdala when healthy participants were asked to regulate negative affect, suggesting top down PFC inhibition of the amygdala. Interestingly, patients with PTSD exhibit less dlPFC recruitment during cognitive reappraisal of emotions as compared with controls [Rabinak et al., 2014]. In healthy individuals, successful regulation of the top-down connectivity between the dmPFC and amygdala, even without neurofeedback, was associated with increases in subjective valence ratings of emotional stimuli [Koush et al., 2015]. Similarly, our collaborators have shown that amygdala downregulation enhances PFC connectivity in healthy individuals [Paret et al., 2016b]—which was found to be unique to the experimental group and did not occur for the sham-neurofeedback group—as well as in BPD patients [Paret et al., 2016a].

DCM Analysis of Amygdala-PFC Effective Connectivity During Neurofeedback

To complement the observed task-based functional connectivity in our gPPI analysis, we computed a DCM analysis to inform directional information flow between the amygdala and PFC during neurofeedback. We tested nine models for the left and right amygdala to the three PFC clusters identified in the gPPI analysis, which was also supposed by anatomical studies of amygdala connectivity [Ghashghaei et al., 2007]. For both the left and right amygdala, family level inferences favored models with PFC driving inputs only (models 7–9). This is in accordance with previous DCM analyses investigating the same nine models during amygdala downregulation in healthy individuals [Paret et al., 2016b]. Additionally, for the left amygdala-right dlPFC, we found a clear distinction for model 9, which was characterized by network input to the dlPFC, with modulation of connectivity from the amygdala to the dlPFC (bottom-up) and from the dlPFC to the amygdala (top-down) via the *regulate* condition ($xP = 0.83$) (see Fig. 6a). We report a less clear distinction for model 9 with regard to the left amygdala- left dmPFC ($xP = 0.40$) and the right amygdala-right dmPFC ($xP = 0.62$) (see Fig. 6b). Similarly, Paret et al. [2016a, b] report a DCM analysis for directional connectivity during amygdala downregulation in healthy individuals, which favored model 7 characterized by predominant information flow from the amygdala to the vmPFC, with the PFC being the entry node to the network.

Critically, previous studies have defined the dlPFC as a central region in emotion regulation [Banks et al., 2007; Etkin et al., 2015; Golkar et al., 2012; Levesque et al., 2003; Stein et al., 2007]. Our results support the hypothesis that emotion regulation is a reciprocal loop of information processing, in which information flows in a bi-directional manner between the amygdala and PFC during amygdala downregulation neurofeedback [Gasquoine, 2014; Kim et al., 2011; Ray and Zald, 2012]. Here, the amygdala is characterized by PFC connections that are bi-directional, pertaining to unique functions among amygdalar subregions [Duvarci and Pare, 2014]. For example, the basolateral amygdala (BLA) has inputs and outputs to the PFC [LeDoux, 2007] and receives feedforward inhibition from the PFC via somatostatin interneurons [Duvarci and Pare, 2014]. Inversely, the centromedial amygdala (CMA) received inputs from the PFC and is involved in the execution of fear responses, with GABAergic outputs to the brainstem and periaqueductal gray involved in descending pain modulation [Duvarci and Pare, 2014; LeDoux, 1998; Milad, 2013]. Critically, the BLA and CMA have been shown to display aberrant connectivity patterns to emotion regulatory prefrontal regions in patients with PTSD

[Brown et al., 2014; Nicholson et al., 2015]. It should also be noted that the observed causal connections between the amygdala and PFC in the current study may be indirect and mediated by other brain regions.

LIMITATIONS AND FUTURE DIRECTIONS

Limitations of our study include a small sample size, where 80% of our sample was receiving psychotropic medication. Additionally, warranting a larger sample, the dissociative subtype of PTSD should be examined separately. Furthermore, we cannot conclude that the observed results are a direct effect of neurofeedback from the amygdala, as no sham neurofeedback regions were included. Future studies will include a second neurofeedback region-of-interest (i.e., prefrontal emotion regulation areas), in which we will examine neural changes as a result of upregulating this region. As a control comparison, we will then correlate observed neuronal effects as a result of regulating the amygdala as compared with regulating prefrontal emotion regulatory regions in order to be able to conclude that the observed effects are site specific [Rance et al., 2014]. Nevertheless, the current findings represent an important first step in the elucidating critical emotion dysregulation mechanisms underlying PTD with regard to amygdala neurofeedback.

CONCLUSION

In summary, PTSD patients were able to downregulate their amygdala activation during trauma provocation, which was sustained during the transfer run without neurofeedback. Downregulation of amygdala activity during neurofeedback training was associated with enhanced activation in PFC regions associated with emotion regulation as well as increased task-based connectivity to the PFC. Effective connectivity analyses suggested that amygdala regulation involves both top-down and bottom-up information flow with regard to observed PFC-amygdala connectivity. Moreover, dissociative symptoms were correlated negatively to emotion regulation PFC/rostral ACC activity as well as with activation in the insula during the transfer run. Taken together, these results support the hypothesis that neural functioning among patients with PTSD is characterized by attenuated prefrontal inhibition on the limbic system, resulting in emotional dysregulation, and suggests that amygdala neurofeedback may not only be therapeutic for this patient group but may also be used as an adjunctive future treatment.

REFERENCES

Admon R, Milad MR, Hendler T (2013): A causal model of posttraumatic stress disorder: Disentangling predisposed from acquired neural abnormalities. Trends Cogn Sci 17:337–347.

Aghajani M, Veer IM, van Hoof MJ, Rombouts SA, van der Wee NJ, Vermeiren RR (2016): Abnormal functional architecture of amygdala-centered networks in adolescent posttraumatic stress disorder. Hum Brain Mapp 37:1120–1135.

Aupperle RL, Melrose AJ, Stein MB, Paulus MP (2012): Executive function and PTSD: Disengaging from trauma. Neuropharmacology 62:686–694.

Banks SJ, Eddy KT, Angstadt M, Nathan PJ, Luan Phan K (2007): Amygdala-frontal connectivity during emotion regulation. Soc Cogn Affect Neurosci 2:303–312.

Beck AT, Guth D, Steer RA, Ball R (1997): Screening for major depression disorders in medical inpatients with the beck depression inventory for primary care. Behav Res Ther 35: 785–791.

Bernstein DP, Stein JA, Newcomb MD, Walker E, Pogge D, Ahluvalia T, Stokes J, Handelsman L, Medrano M, Desmond D, Zule W (2003): Development and validation of a brief screening version of the Childhood Truama Questionnaire. Child Abuse Negl 27:169–190.

Birn RM, Patriat R, Phillips ML, Germain A, Herringa RJ (2014): Childhood maltreatment and combat posttraumatic stress differentially predict fear-related fronto-subcortical connectivity. Depress Anxiety 31:880–892.

Blake DD, Weathers FW, Nagy LM, Kaloupek DG, Gusman FD, Charney DS, Keane TM (1995): The development of a Clinician-Administered PTSD Scale. J Trauma Stress 8:75–90.

Briere J, Weathers FW, Runtz M (2005): Is dissociation a multidimensional construct? Data from the multiscale dissociation inventory. J Trauma Stress 18:221–231.

Brown VM, LaBar KS, Haswell CC, Gold AL, Beall SK, Van Voorhees E, Marx CE, Calhoun PS, Fairbank JA, Green KT, Tupler LA, Weiner RD, Beckham JC, Brancu M, Hoerle JM, Pender M, Kudler H, Swinkels CM, Nieuwsma JA, Runnals JJ, Youssef NA, McDonald SD, Davison R, Yoash-Gantz R, Taber KH, Hurley R, McCarthy G, Morey RA (2014): Altered resting-state functional connectivity of basolateral and centromedial amygdala complexes in posttraumatic stress disorder. Neuropsychopharmacology 39:361–369.

Bruce SE, Buchholz KR, Brown WJ, Yan L, Durbin A, Sheline YI (2013): Altered emotional interference processing in the amygdala and insula in women with Post-Traumatic Stress Disorder. NeuroImage Clin 2:43–49.

Brühl AB, Scherpiet S, Sulzer J, Stämpfli P, Seifritz E, Herwig U (2014): Real-time neurofeedback using functional MRI could improve down-regulation of amygdala activity during emotional stimulation: A proof-of-concept study. Brain Topogr 27:138–148.

Bryant R, Kemp AH, Felmingham KL, Liddell B, Olivieri G, Peduto A, Gordon E, Williams LM (2008): Enhanced amygdala and medial prefrontal activation during nonconscious processing of fear in posttraumatic stress disorder: An fMRI study. Hum Brain Mapp 29:517–523.

Craig ADB (2009): How do you feel - now? The anterior insula and human awareness. Nat Rev Neurosci 10:59–70.

Critchley HD, Wiens S, Rotshtein P, Ohman A, Dolan RJ (2004): Neural systems supporting interoceptive awareness. Nat Neurosci 7:189–195.

Doll A, Hölzel BK, Bratec SM, Boucard CC, Xie X, Wohlschläger AM, Sorg C (2016): Mindful attention to breath regulates emotions via increased amygdala–prefrontal cortex connectivity. Neuroimage 134:305–313.

Duvarci S, Pare D (2014): Amygdala microcircuits controlling learned fear. Neuron 82:966–980.

Emmert K, Breimhorst M, Bauermann T, Birklein F, Rebhorn C, Van De Ville D, Haller S (2016): Active pain coping is associated with the response in real-time fMRI neurofeedback during pain. Brain Imaging Behav 1–10.

Etkin A, Wager TD (2007): Functional neuroimaging of anxiety: A meta-analysis of emotional processing in PTSD, social anxiety disorder, and specific phobia. Am J Psychiatry 164:1476–1488.

Etkin A, Egner T, Peraza DM, Kandel ER, Hirsch J (2006): Resolving emotional conflict: A role for the rostral anterior cingulate cortex in modulating activity in the amygdala. Neuron 51: 871–882.

Etkin A, Büchel C, Gross JJ (2015): The neural bases of emotion regulation. Nat Rev Neurosci 16:693–700.

Etkin A, Egner T, Kalisch R (2011): Emotional processing in anterior cingulate and medial prefrontal cortex. Trends Cogn Sci 15: 85–93.

First MB (1997): User's Guide for the Structured Clinical Interview for DSM-IV Axis I Disorders SCID-I: Clinician Version. Washington, DC: American Psychiatric Press.

Fonzo GA, Simmons AN, Thorp SR, Norman SB, Paulus MP, Stein MB (2010): Exaggerated and disconnected insular-amygdalar blood oxygenation level-dependent response to threat-related emotional faces in women with intimate-partner violence posttraumatic stress disorder. Biol Psychiatry 68:433–441.

Frank DW, Dewitt M, Hudgens-Haney M, Schaeffer DJ, Ball BH, Schwarz NF, Hussein AA, Smart LM, Sabatinelli D (2014): Emotion regulation: Quantitative meta-analysis of functional activation and deactivation. Neurosci Biobehav Rev 45: 202–211.

Frewen PA, Dozois DJA, Neufeld RWJ, Densmore M, Stevens TK, Lanius RA (2011): Neuroimaging social emotional processing in women: fMRI study of script-driven imagery. Soc Cogn Affect Neurosci 6:375–392.

Friston KJ, Harrison L, Penny W (2003): Dynamic causal modelling. Neuroimage 19:1273–1302.

Gasquoine PG (2014): Contributions of the insula to cognition and emotion. Neuropsychol Rev 24:77–87.

Gerin MI, Fichtenholtz HP, Roy A, Walsh CJ, Krystal JH, Southwick S, Hampson MP (2016): Real-time fMRI neurofeedback with war veterans with chronic PTSD: a feasibility study. Front Psychiatry 7:111.

Gläscher J (2009): Visualization of group inference data in functional neuroimaging. Neuroinformatics 1:73–82.

Ghashghaei HT, Hilgetag CC, Barbas H (2007): Sequence of information processing for emotions based on the anatomic dialogue between prefrontal cortex and amygdala. Neuroimage 34:905–923.

Goebel R (2014): Dynamic ROIs. TBV Users Guide. Available at http://download.brainvoyager.com/tbv/TBVUsersGuide/Neurofeedback/DynamicROIs.html

Golkar A, Lonsdorf TB, Olsson A, Lindstrom KM, Berrebi J, Fransson P, Schalling M, Ingvar M, Öhman A (2012): Distinct contributions of the dorsolateral prefrontal and orbitofrontal cortex during emotion regulation. PLoS One 7:e48107.

Hayes JP, Hayes SM, Mikedis AM (2012): Quantitative meta-analysis of neural activity in posttraumatic stress disorder. Biol Mood Anxiety Disord 2:9.

Hopper JW, Frewen PA, van der Kolk BA, Lanius RA (2007): Neural correlates of reexperiencing, avoidance, and dissociation in PTSD: Symptom dimensions and emotion dysregulation in responses to script-driven trauma imagery. J Traum Stress 20:713–725.

Huang M-X, Yurgil KA, Robb A, Angeles A, Diwakar M, Risbrough VB, Nichols SL, McLay R, Theilmann RJ, Song T, Huang CW, Lee RR, Baker DG (2014): Voxel-wise resting-state MEG source magnitude imaging study reveals neurocircuitry abnormality in active-duty service members and veterans with PTSD. NeuroImage Clin 5:408–419.

Ichesco E, Schmidt-Wilcke T, Bhavsar R, Clauw DJ, Peltier SJ, Kim JN, Vitaly H, Johnson P, Kairys AE, Williams DA, Harris RE (2014): Altered resting state connectivity of the insular cortex in individuals with fibromyalgia. J Pain 15:815–882.

Kerr DL, McLaren DG, Mathy RM, Nitschke JB (2012): Controllability modulates the anticipatory response in the human ventromedial prefrontal cortex. Front Psychol 3:1–11.

Keynan JN, Meir-Hasson Y, Gilam G, Cohen A, Jackont G, Kinreich S, Ikar L, Or-Borichev A, Etkin A, Gyurak A, Klovatch I, Intrator N, Hendler T (2016): Limbic activity modulation guided by fMRI-inspired EEG improves implicit emotion regulation. Biol Psychiatry 1–7.

Kim MJ, Loucks RA, Palmer AL, Brown AC, Solomon KM, Marchante AN, Whalen PJ (2011): The structural and functional connectivity of the amygdala: From normal emotion to pathological anxiety. Behav Brain Res 223:403–410.

Kluetsch RC, Ros T, Théberge J, Frewen PA, Calhoun VD, Schmahl C, Jetly R, Lanius RA (2014): Plastic modulation of PTSD resting-state networks and subjective wellbeing by EEG neurofeedback. Acta Psychiatr Scand 130:123–136.

Koch SB, Zuiden M, Nawijn L, Frijling JL, Veltman DJ, Olff M (2016): Aberrant resting-state brain activity in posttraumatic stress disorder: A meta-analysis and systematic review. Depress Anxiety.

Koush Y, Rosa MJ, Robineau F, Heinen K, Rieger SW, Weiskopf N, Vuilleumier P, Van De Ville D, Scharnowski F (2013): Connectivity-based neurofeedback: Dynamic causal modeling for real-time fMRI. Neuroimage 81:422–430.

Koush Y, Meskaldji D-E, Pichon S, Rey G, Rieger SW, Linden DEJ, Van De Ville D, Vuilleumier P, Scharnowski F (2015): Learning control over emotion networks through connectivity-based neurofeedback. Cereb Cortex (in press).

Kurth F, Eickhoff SB, Schleicher A, Hoemke L, Zilles K, Amunts K (2010): Cytoarchitecture and probabilistic maps of the human posterior insular cortex. Cereb Cortex 20:1448–1461.

Lanius RA, Vermetten E, Loewenstein RJ, Brand B, CS, Bremner JD, Spiegel D (2010): Emotion modulation in PTSD: Clinical and neurobiological evidence for a dissociative subtype. Am J Psychiatry 167:640–647.

Lanius RA, Frewen PA, Tursich M, Jetly R, Mckinnon MC (2015): Restoring large-scale brain networks in PTSD and related disorders: A proposal for neuroscientifically-informed treatment interventions. Eur J Psychotraumatol 6:10.

LeDoux J (1998). Fear and the brain: where have we been, and where are we going? Biol Psychiatry 44:1229–1238.

LeDoux J (2007): The amygdala. Curr Biol 17:868–874.

Levesque J, Euge F, Joanette Y, Paquette V, Mensour B, Beaudoin G, Leroux J, Bourgouin P (2003): Neural circuitry underlying voluntary suppression of sadness. Biol Psychiatry 53:502–510.

Maldjian JA, Laurienti PJ, Burdette JB, Kraft RA (2003): An automated method for neuroanatomic and cytoarchitectonic atlas-based interrogation of fMRI data sets. NeuroImage 19: 1233–1239.

McLaren DG, Ries ML, Xu G, Johnson SC (2012): A generalized form of context-dependent psychophysiological interactions

(gPPI): A comparison to standard approaches. Neuroimage 61: 1277–1286.
Menon V, Uddin LQ (2010): Saliency, switching, attention and control: A network model of insula function. Brain Struct Funct 214:655–667.
Mickleborough MJS, Daniels JK, Coupland NJ, Kao R, Williamson PC, Lanius UF, Hegadoren K, Schore A, Densmore M, Stevens T, Lanius RA (2011): Effects of trauma-related cues on pain processing in posttraumatic stress disorder: An fMRI investigation. J Psychiatry Neurosci 36:6–14.
Milad M (2013): Amygdala metabolism and associative fear learning in PTSD. Biol Psychiatry 73:124S–124S.
Nicholson AA, Densmore M, Frewen PA, Théberge J, Neufeld RWJ, McKinnon MC Lanius (2015): The dissociative subtype of posttraumatic stress disorder: unique resting-state functional connectivity of basolateral and centromedial amygdala complexes. Neuropsychopharmacology 2317–2326.
Nicholson AA, Sapru I, Densmore M, Frewen PA, Neufeld RWJ, Theberge J, McKinnon MC, Lanius RA (2016a): Unique insula subregion resting-state functional connectivity with amygdala complexes in posttraumatic stress disorder and its dissociative subtype. Psychiatry Res Neuroimaging 2:61–72.
Nicholson A, Ros T, Frewen PA, Densmore M, Théberge J, Kluetsch RC, Lanius RA (2016b): Alpha oscillation neurofeedback modulates amygdala complex connectivity and arousal in posttraumatic stress disorder. NeuroImage Clin 12:506–516.
Paret C, Kluetsch R, Ruf M, Demirakca T, Hoesterey S, Ende G, Schmahl C (2014): Down-regulation of amygdala activation with real-time fMRI neurofeedback in a healthy female sample. Front Behav Neurosci 8:299.
Paret C, Kluetsch R, Zaehringer J, Ruf M, Demirakca T, Bohus M, Ende G, Schmahl C (2016a): Alterations of amygdala-prefrontal connectivity with real-time fMRI neurofeedback in BPD patients. Soc Cogn Affect Neurosci 11:952–960.
Paret C, Ruf M, Fungisai Gerchen M, Kluetsch R, Demirakca T, Jungkunz M, Bertsch K, Schmahl C, Ende G (2016b): fMRI neurofeedback of amygdala response to aversive stimuli enhances prefrontal-limbic brain connectivity. Neuroimage 125:182–188.
Patel R, Spreng RN, Shin LM, Girard TA (2012): Neurocircuitry models of posttraumatic stress disorder and beyond: A meta-analysis of functional neuroimaging studies. Neurosci Biobehav Rev 36:2130–2142.
Peres JFP, Newberg AB, Mercante JP, Simão M, Albuquerque VE, Peres MJP, Nasello AG (2007): Cerebral blood flow changes during retrieval of traumatic memories before and after psychotherapy: A SPECT study. Psychol Med 37:1481–1491.
Pitman RK, Rasmusson AM, Koenen KC, Shin LM, Orr SP, Gilbertson MW, Milad MR, Liberzon I (2012): Biological studies of post-traumatic stress disorder. Nat Rev Neurosci 13: 769–787.
Rabellino D, Densmore M, Frewen PA, Théberge J, Lanius RA (2015a): The innate alarm circuit in post-traumatic stress disorder: Conscious and subconscious processing of fear- and trauma-related cues. Psychiatry Res - Neuroimaging 248: 142–150.
Rabellino D, Tursich M, Frewen PA, Daniels JK, Densmore M, Théberge J, Lanius RA (2015b): Intrinsic Connectivity Networks in post-traumatic stress disorder during sub- and supraliminal processing of threat-related stimuli. Acta Psychiatr Scand 132;365–378.
Rabinak CA, Angstadt M, Welsh RC, Kenndy AE, Lyubkin M, Martis B, Luan Phan K (2011): Altered amygdala resting-state functional connectivity in post-traumatic stress disorder. Front Psychiatry 2:62.
Rabinak CA, Macnamara A, Kennedy AE, Angstadt M, Stein MB, Liberzon I, Phan KL (2014): Focal and aberrant prefrontal engagement during emotion regulation in veterans with posttraumatic stress disorder. Depress Anxiety 861:851–861.
Rance M, Ruttorf M, Nees F, Rudi Schad L, Flor H (2014): Real time fMRI feedback of the anterior cingulate and posterior insular cortex in the processing of pain. Hum Brain Mapp 5798:5784–5798.
Ravindran LN, Stein MB (2009): Pharmacotherapy of PTSD: Premises, principles, and priorities. Brain Res 1293:24–39.
Ray RD, Zald DH (2012): Anatomical insights into the interaction of emotion and cognition in the prefrontal cortex. Neurosci Biobehav Rev 36:479–501.
Reiter K, Andersen SB, Carlsson J (2016): Neurofeedback treatment and posttraumatic stress disorder. J Nerv Ment Dis 204: 69–77.
Ronzoni G, del Arco A, Mora F, Segovia G (2016): Enhanced noradrenergic activity in the amygdala contributes to hyperarousal in an animal model of PTSD. Psychoneuroendocrinology 70:1–9.
Roy AK, Shehzad Z, Margulies DS, Kelly a. MC, Uddin LQ, Gotimer K, Biswal BB, Castellanos FX, Milham MP (2009): Functional connectivity of the human amygdala using resting state fMRI. Neuroimage 45:614–626.
Sadeh N, Spielberg JM, Warren SL, Miller GA, Heller W (2014): Aberrant neural connectivity during emotional processing associated with posttraumatic stress. Clin Psychol Sci 2: 748–755.
Sarkheil P, Zilverstand A, Kilian-Hütten N, Schneider F, Goebel R, Mathiak K (2015): fMRI feedback enhances emotion regulation as evidenced by a reduced amygdala response. Behav Brain Res 281:326–332.
Scheinost D, Stoica T, Saksa J, Papademetris X, Constable RT, Pittenger C, Hampson M (2013): Orbitofrontal cortex neurofeedback produces lasting changes in contamination anxiety and resting-state connectivity. Transl Psychiatry 3:e250.
Seedat S, Warwick J, Van Heerden B, Hugo C, Zungu-Dirwayi N, Van Kradenburg J, Stein DJ (2004): Single photon emission computed tomography in posttraumatic stress disorder before and after treatment with a selective serotonin reuptake inhibitor. J Affect Disord 80:45–53.
Shin LM, Liberzon I (2010): The neurocircuitry of fear, stress, and anxiety disorders. Neuropsychopharmacology 35:169–191.
Sitaram R, Caria A, Veit R, Gaber T, Rota G, Kuebler A, Birbaumer N (2007): FMRI brain-computer interface: A tool for neuroscientific research and treatment. Comput Intell Neurosci 2007:
Sripada RK, King AP, Garfinkel SN, Wang X, Sripada CS, Welsh RC, Liberzon I (2012): Altered resting-state amygdala functional connectivity in men with posttraumatic stress disorder. J Psychiatry Neurosci 37:241–249.
Stein JL, Wiedholz LM, Bassett DS, Weinberger DR, Zink CF, Mattay VS, Meyer-Lindenberg A (2007): A validated network of effective amygdala connectivity. Neuroimage 36:736–745.
Stephan KE, Penny WD, Daunizeau J, Moran RJ, Friston KJ (2009): Bayesian model selection for group studies. Neuroimage 46: 1004–1017.
Stephan KE, Penny WD, Moran RJ, den Ouden HEM, Daunizeau J, Friston KJ (2010): Ten simple rules for dynamic causal modeling. Neuroimage 49:3099–3109.
Stevens JS, Jovanovic T, Fani N, Ely TD, Glover EM, Bradley B, Ressler KJ (2013): Disrupted amygdala-prefrontal functional

connectivity in civilian women with posttraumatic stress disorder. J Psychiatr Res 47:1469–1478.

Taylor KS, Seminowicz DA, Davis KD (2009): Two systems of resting state connectivity between the insula and cingulate cortex. Hum Brain Mapp 30:2731–2745.

Weston CSE (2014): Posttraumatic stress disorder: A theoretical model of the hyperarousal subtype. Front Psychiatry 5:1–20.

Williams LM, Kemp AH, Felmingham K, Barton M, Olivieri G, Peduto A, Gordon E, Bryant RA (2006): Trauma modulates amygdala and medial prefrontal responses to consciously attended fear. Neuroimage 29:347–357.

Wolf RC, Herringa RJ (2016): Prefrontal-amygdala dysregulation to threat in pediatric post-traumatic stress disorder. Neuropsychopharmacology 41:1–10.

Yehuda R, Hoge CW, McFarlane AC, Vermetten E, Lanius RA, Nievergelt CM, Hobfoll SE, Koenen KC, Neylan TC, Hyman SE (2015): Post-traumatic stress disorder. Nat Rev Dis Prim 15057.

Young KD, Zotev V, Phillips R, Misaki M, Yuan H, Drevets WC, Bodurka J (2014): Real-time fMRI neurofeedback training of amygdala activity in patients with major depressive disorder. PLoS One 9:e88785.

Zhu Y, Du R, Zhu Y, Shen Y, Zhang K, Chen Y, Song F, Wu S, Zhang H, Tian M (2016). PET Mapping of Neurofunctional Changes in a Post-traumatic Stress Disorder Model. J Nucl Med 57:1474.

Zotev V, Krueger F, Phillips R, Alvarez RP, Simmons WK, Bellgowan P, Drevets WC, Bodurka J (2011): Self-regulation of amygdala activation using real-time FMRI neurofeedback. PLoS One 6:e24522.

Zotev V, Phillips R, Yuan H, Misaki M, Bodurka J (2014): Self-regulation of human brain activity using simultaneous real-time fMRI and EEG neurofeedback. Neuroimage 85: 985–995.

Zotev V, Yuan H, Misaki M, Phillips R, Young KD, Feldner MT, Bodurka J (2016): Correlation between amygdala BOLD activity and frontal EEG asymmetry during real-time fMRI neurofeedback training in patients with depression. NeuroImage Clin 11:224–238.